Molecular Biology of the Cell
Vol. 21, 4387–4399, December 15, 2010

Podoplanin Associates with CD44 to Promote Directional Cell Migration

Ester Martín-Villar,* Beatriz Fernández-Muñoz,†‡ Maddy Parsons,* Maria M. Yurrita,† Diego Megías,§ Eduardo Pérez-Gómez,† Gareth E. Jones,* and Miguel Quintanilla†

*Randall Division of Cell and Molecular Biophysics, King's College London, Guy's Campus, SE1UL, UK; †Instituto de Investigaciones Biomédicas Alberto Sols, Consejo Superior de Investigaciones Científicas (CSIC)-Universidad Autónoma de Madrid (UAM) and §Centro Nacional de Investigaciones Oncológicas, 28029 Madrid, Spain

Submitted June 7, 2010; Revised September 27, 2010; Accepted October 12, 2010
Monitoring Editor: Jonathan Chernoff

Podoplanin is a transmembrane glycoprotein up-regulated in different human tumors, especially those derived from squamous stratified epithelia (SCCs). Its expression in tumor cells is linked to increased cell migration and invasiveness; however, the mechanisms underlying this process remain poorly understood. Here we report that CD44, the major hyaluronan (HA) receptor, is a novel partner for podoplanin. Expression of the CD44 standard isoform (CD44s) is coordinately up-regulated together with that of podoplanin during progression to highly aggressive SCCs in a mouse skin model of carcinogenesis, and during epithelial-mesenchymal transition (EMT). In carcinoma cells, CD44 and podoplanin colocalize at cell surface protrusions. Moreover, CD44 recruitment promoted by HA-coated beads or cross-linking with a specific CD44 antibody induced corecruitment of podoplanin. Podoplanin–CD44s interaction was demonstrated both by coimmunoprecipitation experiments and, in vivo, by fluorescence resonance energy transfer/fluorescence lifetime imaging microscopy (FRET/FLIM), the later confirming its association on the plasma membrane of cells with a migratory phenotype. Importantly, we also show that podoplanin promotes directional persistence of motility in epithelial cells, a feature that requires CD44, and that both molecules cooperate to promote directional migration in SCC cells. Our results support a role for CD44-podoplanin interaction in driving tumor cell migration during malignancy.

INTRODUCTION

Podoplanin (PA2.26 antigen, Aggrus, or T1α) is a type I transmembrane sialomucin up-regulated in different types of cancer, such as squamous cell carcinomas (SCCs) and testicular germ cell tumors (see Wicki and Christofori, 2007 for a review). Several reports support the involvement of podoplanin in malignant progression. First, it has been shown that podoplanin/Aggrus induces platelet aggregation facilitating tumor-platelet aggregate formation and metastasis (Kunita *et al*., 2007). Second, we found that podoplanin/PA2.26 antigen promotes either cell scattering or a full epithelial–mesenchymal transition (EMT) associated with cell migration, invasion, and metastasis (Scholl *et al*., 1999; Scholl *et al*., 2000; Martin-Villar *et al*., 2005; Martin-Villar *et al*., 2006). Third, Wicki and colleagues reported that podoplanin can promote collective tumor cell migration and invasion in a pancreatic cancer mouse model (Wicki *et al*., 2006). Because podoplanin lacks any obvious enzymatic motif within its structure, all these activities have to be mediated by protein–protein interactions, hence the need to identify its binding partners. Thus, the binding of podoplanin ectodomain to C-type lectin-like receptor 2 (CLEC-2) is involved in podoplanin-induced platelet aggregation (Kato *et al*., 2008), a process which is attenuated by the interaction of podoplanin with CD9 tetraspanin (Nakazawa *et al*., 2008). In addition, podoplanin-induced EMT is linked to RhoA activation and requires the association of the podoplanin cytoplasmic tail with ezrin and/or moesin, members of the ERM (ezrin, radixin, moesin) protein family of membrane-cytoskeleton linkers (Martin-Villar *et al*., 2006).

In this report, we identify the standard isoform of CD44 (CD44s) as a novel partner for podoplanin. CD44 is a widely distributed and highly polymorphic type I transmembrane glycoprotein. Although it is encoded by a single gene, the region comprising the extracellular domain includes 10 vari-

This article was published online ahead of print in *MBoC in Press* (http://www.molbiolcell.org/cgi/doi/10.1091/mbc.E10–06–0489) on October 20, 2010.

‡ Present address for B.F.-M.: Centro de Biologia Molecular Severo Ochoa, UAM, Cantoblanco, 28049 Madrid, Spain.

Address correspondence to: Ester Martín-Villar (ester.martin@kcl.ac.uk) or Miguel Quintanilla (mquintanilla@iib.uam.es).

Abbreviations used: CD44s, CD44 standard isoform; CD44v, CD44 variant isoform; eGFP, enhanced green fluorescent protein; EMT, epithelial to mesenchymal transition; ERM, ezrin, radixin, moesin; FRET-FLIM, fluorescence resonance energy transfer–fluorescence lifetime imaging microscopy; HA, hyaluronan; SCC, squamous cell carcinomas.

able exons (v1–10; CD44v) that can be alternatively spliced, generating multiple isoforms (Screaton *et al*., 1992). CD44s lacks all the variable exons and has a widespread tissue distribution. An additional source of variation for all the CD44 isoforms is glycosylation, which differ depending on the type and activation state of the cell (Hathcock *et al*., 1993; Skelton *et al*., 1998). CD44 functions as the major hyaluronan (HA) receptor and mediates cell adhesion and migration in a variety of pathophysiological processes, including tumor metastasis, wound healing, and inflammation (Isacke and Yarwood, 2002; Marhaba and Zoller, 2004). CD44 can also act as a coreceptor modulating signal transduction through cell-surface tyrosine kinase receptors. Interestingly, this function depends on the ability of CD44 to bind ERM proteins through its cytoplasmic tail (Ponta *et al*., 2003). The podoplanin–CD44s interaction described here provides a new mechanism by which both of these glycoproteins cooperate to promote cell migration and tumor progression.

MATERIALS AND METHODS

Cell Culture

Epidermal cell lines (Supplemental Table S1) were grown as described before (Quintanilla *et al*., 2003). MDCK- and MCA3D-podoplanin cell transfectants have been described previously (Scholl *et al*., 1999; Scholl *et al*., 2000; Martin-Villar *et al*., 2006). HEK293T, HT1080, and MDCK-Snail1, -Snail2, and -E47 cells were a generous gift from Dr. Amparo Cano (Instituto de Investigaciones Biomedicas Alberto Sols, Madrid, Spain). HN5 cells were kindly provided by Dr. Marcella Flinterman (Oral Pathology Department, King's College London, London, UK). HaCaT, HEK293T, HT1080, HN5, and MDCK cells were grown in Dulbecco's Modified Eagle Medium (DMEM) supplemented with 10% fetal calf serum, (Biosera, Sussex UK) 1% Pen-Strep (Sigma, Dorset, UK) and L-glutamine (PAA Laboratories GmbH, Germany).

cDNA Constructs and RNA Interference

Full-length wild-type human podoplanin and mutant constructs subcloned into the pcDNA3 and pEGFP vectors have been described elsewhere (Martin-Villar *et al*., 2006). Human podoplanin and CD44s tagged with Hae and Flag at the C terminus and mRFP-tagged CD44s constructs were obtained by PCR amplification using primers that carry convenient restriction sites to facilitate subcloning into pcDNA3-Hae/Flag and pmRFP-N1 vectors. Oligonucleotides used for amplification of all these constructs are described in Table S2 in the Supplemental material.

Short-hairpin RNAs (shRNAs) targeting human podoplanin mRNA were cloned into pLKO.1 vector (Addgene, Cambridge, UK). Lentiviral supernatants were produced in HEK293T cells by cotransfection of pCMV-d8.9 (packaging plasmid), pMD2G (envelope plasmid), and pLKO.1 including targeting sequences and collected after 24 and 48 h. HN5 cells were grown at (~70%) confluence and infected with lentiviral supernatants. After 48 h, infected HN5 cells were selected by addition of 1.4 μg/ml puromycin (Sigma). Both podoplanin target sequences, 5′AAGACCGTTCACCAGACTTGG3′ (podo sh1) and 5′AACACTGGACCATTGGATCGA3′ (podo sh2), successfully knocked-down expression of the target gene. For control experiments, cells were infected with viral vectors containing scrambled shRNA (Addgene; ID 1864).

For CD44 down-regulation in MDCK cells following small interfering (siRNA) oligonucleotides were used: 5′ GACCACGACUCAUCGGUUC dT dT3′ and GAACCGAUGAGUCGUGGUC dT dT3′. siRNA against Firefly luciferase GL3 was used as negative control (Elbashir *et al*., 2001).

For human CD44 knockdown the following siRNAs were used: 5′GUAUGACACAAUAUUGCUUC dT dT3′ and 5′GAAGCAAUAUGUGUCAUAC dT dT3′ (Roscic-Mrkic *et al*., 2003). Control oligonucleotides where purchased from Ambion (Warrington, UK; Silencer Negative control #1, AM4611). Annealed siRNA oligonucleotides were transfected with 100 μM oligofectamine (Invitrogen, Paisley, UK) in Opti-MEM reduced-serum medium (Invitrogen). Cells were incubated at 37oC for 6 h before the addition of FBS to 10%. All the assays were conducted at 48–72 h after transfection.

Mouse Skin Carcinogenesis

The two-stage mouse skin carcinogenesis (a single DMBA application followed by twice weekly applications of TPA for 16 wk) was performed following standard protocols (Perez-Gomez *et al*., 2007). Tumors were collected at different time periods after initiation (papillomas at 30 wk and SCCs at 43 wk) and processed for Western blotting. Tumors were histologically typed by H&E staining of paraffin sections and characterized by the expression of the following differentiation/progression markers: keratins K1 and K10, which are lost in SCCs; the extracellular matrix component SPARC, which is induced during progression from papillomas to SCCs; as well as the E-cadherin transcriptional repressor Snail1 and the enzyme lysyl oxidase-like 2, which accumulate in poorly differentiated SCCs, as previously described (Perez-Gomez *et al*., 2007).

RT-PCR

Reverse transcription was performed as previously described (Martin-Villar *et al*., 2006). For CD44 analyses specific primers were designed to amplify both human and canine genes: 5′-TATTGCTTCAATGCTTCAGCTCCA-3′ and 5′-AGGTTGTGTTTGCTCCACCTTCTTGAC-3′. PCR products were obtained after 35 cycles of amplification with an annealing temperature of 60°C.

Western Blot and Coimmunoprecipitation Experiments

For detection of podoplanin and CD44 in Western blots, cells or tissues were lysed in buffer RIPA (0.1% SDS, 0.5% sodium deoxycholate, 1% Nonidet P-40, 150 mM NaCl, 50 mM Tris-HCl pH 8.0) and a cocktail of protease inhibitors (1 mM phenylmethylsulfonyl fluoride, 2 μg/ml aprotinin and 2 μg/ml leupeptin). Samples containing the same amount of protein (10–30 μg) were run on 10% SDS-PAGE and transferred to Immobilon P membranes (Millipore, Bedford, MA). Filters were then immunoblotted with the following Abs: anti mouse podoplanin (PA2.26 mAb; previously described in Gandarillas *et al*., 1997), anti human podoplanin (NZ1 mAb purchased from Acris Antibodies, Herford, Germany), rat mAb IM7 against CD44 ectodomain (generously provided by Dr Helen Yarwood; The Institute of Cancer Research, London, UK), rabbit polyclonal Ab raised to the COOH terminal region of CD44 (CD44cyto, Abcam, Cambridge, UK), and mouse mAbs against α-tubulin, β-actin (Sigma) and GAPDH (Roche Diagnostics, Welwyn Garden City, UK).

For coimmunoprecipitation experiments HEK293T cells were transiently cotransfected with expression vectors using Effectene (Qiagen, Crawley, UK), as indicated by the manufacturer. After 24 h, cells were lysed in IP buffer (50 mM Tris-HCl pH 8.0, 100 mM NaCl, EDTA 5 mM, 0.5% Triton X-100, 10% glycerol) containing Complete Protease Inhibitors Cocktail Tablets (Roche Diagnostics). Tagged CD44s-Hae or podoplanin-Flag proteins were immunoprecipitated using anti-Hae (Roche Diagnostics) or anti-Flag (Sigma) mAbs linked to protein A/G resin (Alpha Diagnostic, TX), respectively. After incubation with 500–750 μg of cell lysates for 2h at 4°C, the resin was then washed five times with lysis buffer, and the coimmunoprecipitates were eluted in 1× Laemmli Buffer. Immunoprecipitation of endogenous podoplain in CarC cells was performed using the PA2.26 mAb for mouse podoplanin and the coimmunoprecipitated products were detected by using the rat mAb IM7 against the CD44 ectodomain.

Coimmunoprecipitation assays of podoplanin-eGFP tagged constructs were performed using an anti-GFP antibody-conjugated resin. The resin was made by cross-linking a GFP polyclonal antibody (MBL International, Woburn, MA) to the protein G beads using a Seize X protein G immunoprecipitation kit purchased from Pierce Biotechnology (Leicestershire, UK). Coimmunoprecipitation was done following the protocol provided by the manufacturer.

Bead and Antibody-Mediated Clustering Assays

Bead coating and incubation were performed as previously described (del Pozo *et al*., 2004). Briefly, 5-μm polystyrene beads (Duke Scientific Corporation, Palo Alto, California) were washed in PBS and incubated with 5 mg/ml BSA or 1 mg/ml high molecular mass HA (Sigma, H7630). Beads were left overnight at 4°C to allow even protein binding, washed three times, and resuspended in PBS to form a 50% slurry final concentration. Coating efficiency of beads with HA was also tested by incubating the beads with fluorescently labeled HA (FITC-HA). Cells plated onto coverslips were incubated with 5 μl/ml coated-beads in growth media and incubated at 37°C for 15–30 min. Cells were then washed three times in medium and fixed for immunofluorescence analysis.

Antibody-mediated clustering assays were performed as described previously (Clark *et al*., 2005). HN5 cells were platted on glass coverslips in DMEM. To cluster CD44, CD44 mAb HP2/9 (generously provided by Dr. Francisco Sánchez-Madrid; Centro Nacional de Investigaciones Cardiovasculares, Madrid, Spain) was incubated with cells in serum-free medium at a concentration of 1 μg/ml for 1 h at 37°C. After three washes with warm PBS to remove all nonbound Ab, a Cy3-labeled secondary Fc-specific Ab (2 μg/ml), was added for 1 h. Under these conditions the secondary Ab induces the cross-linking of the primary Ab through its Fc-tail. This results in clustering the protein of interest. After washing the samples three times with warm PBS, cells were fixed and processed for immunofluorescence as described below.

FRET-FLIM Microscopy

FLIM was used to measure FRET between podoplanin eGFP constructs and CD44s-mRFP in MDCK cotransfected cells. Podoplanin-eGFP and CD44-mRFP constructs (at a Podoplanin-eGFP to CD44s-mRFP ratio of 1:3) or with Podoplanin-eGFP alone were cotransfected using FuGene6 (Roche) according to the manufacturer's instructions. Cells were left to express the constructs for 48 h and then fixed with 4% paraformaldehyde in PBS for 20 min, permeabilized with 0.01% Triton X-100/PBS for 10 min, and incubated with 1 mg/ml fresh Sodium Borohydride/PBS for 10 min at room temperature.

FLIM measurements were performed on a multiphoton microscope via time-correlated single-photon counting (for details see Parsons *et al*., 2008). FLIM analysis to calculate eGFP lifetime and FRET efficiency was performed using TRI2 software (developed by Paul Barber, Gray Cancer Institute, London, UK).

Confocal Microscopy and Morphological Analysis

Cells on coverslips were fixed with 3.7% formaldehyde for 30 min and permeabilized with 0.05% Triton-X100/PBS for 10 min. Podoplanin and CD44 staining was carried out using the anti-human podoplanin mAb (NZ-1) and the anti-CD44 HP2/9 mAb. Confocal images were acquired on a Leica TCS-SP2 microscope for Figure 2A or on a NIKON A1 confocal laser-scanning microscope for Figure 2, B and C and Figure 7. Images were assembled using Leica confocal software 2.0 or NIS-Elements AR 3.0.

For morphological analyses cells were allowed to spread for 24 h and then processed for immunofluorescence. The actin cytoskeleton was visualized by staining with Alexa Fluor 568-labeled phalloidin (Invitrogen). Tubulin was detected using a specific mouse anti–α-tubulin Ab (Sigma). Cell area was quantified using the public domain program NIH ImageJ (developed at the US National Institutes of Health).

Cell Migration Assays and Time-Lapse Microscopy

The migratory behavior of the cells was analyzed by using 8-μm pore transwell chambers (Corning, Amsterdam, NE) and in vitro scratch assays. For transwell assays MDCK cells were cotransfected with podoplanin-eGFP or eGFP and CD44 or control siRNA. 2.5×10^4 cells per well were seeded 48 h after transfection in DMEM containing 0.1% FBS and allowed to transmigrate to 10% FBS medium for 12 h at 37°C. Cells on the upper side of the transwell were then removed, and those on the underside were fixed and stained with crystal violet. Cell migration was quantified by counting the number of cells that migrated through the inserts (three different fields per well were counted under a NIKON Eclipse TS100 inverted light microscope, using a ×10 objective).

Random migration analysis in MDCK cells was performed by time-lapse fluorescence microscopy. Cells were sparsely plated, grown in the absence of serum, and imaged overnight. Pictures were taken every 5 min with the ×10 objective of a Leica DMI6000B inverted fluorescence microscope. Migration was analyzed by Imaris 6.4.2 software to obtain cell trajectories and calculate path length, displacement from origin, and average speed (total path length/time). Persistence of migration (directionality) was defined as displacement from origin/total cell path.

For wound healing assays podoplanin- and/or CD44-depleted HN5 cells were plated onto collagen I (BD Biosciences, Oxford, UK)-coated 12-well plates and left for 24 h to form a monolayer. Confluent monolayers were scratched with a tip and cells were imaged in an atmosphere of 5% CO2 at 37°C with a ×5 phase objective and an inverted microscope (Axiovert 100, Carl Zeiss MicroImaging,) equipped with a charge-coupled device camera (Sensicam;PCO) and motorized stage (Ludl). Images of the wounds were collected every 10-min intervals for a period of 18 h. Image acquisition was controlled by ANDOR IQ software. Sequences of images were quantitatively analyzed using ImageJ software. Cell outlines were drawn along the wound edge at time 0 h and 18 h. Migration was quantified by calculating the area between the two outlines. Kinetics of migrating cells along the wound edge were analyzed using the manual tracking tool in Image J and Mathematica 7.0 workbooks (Allen *et al*., 1998). Images and videos were assembled using Image J and Adobe Premiere Pro1.5 software.

Statistics

All experiments were performed at least three times. Data are presented as mean ± SEM. Significance was determined using one-way analysis of variance (ANOVA) followed by Bonferroni's post test or two-tailed Student's *t* test. $p < 0.05$ was considered statistically significant. All statistical analyses were performed using GraphPad Prism 4.0 software.

RESULTS

The Coordinate Expression of Podoplanin and CD44s Correlates with Malignant Progression and EMT

We have previously shown that ectopic expression of podoplanin in epithelial MDCK cells promoted a dramatic change from an epithelial to a fibroblastic-like morphology linked to down-regulation of epithelial genes, such as E-cadherin, and up-regulation of mesenchymal markers, such as fibronectin (Figure S1 in supplementary material; Martin-Villar *et al*., 2006). When the levels of CD44 mRNA and protein were analyzed in MDCK cells expressing podoplanin (MDCK-Podo), a switch in the expression from CD44v isoforms to CD44s was associated with the acquisition of a fibroblastic phenotype (Figure 1A). As shown in Figure 1B, this CD44 isoform switch was also seen in EMTs induced by the overexpression of the E-cadherin repressors Snail 1, Snail 2, and E47 in MDCK cells (Peinado *et al*., 2007).

EMT in mouse skin chemical carcinogenesis is associated with progression from well-differentiated tumors to highly aggressive undifferentiated or spindle cell carcinomas (Akhurst and Balmain, 1999). Because podoplanin was identified as a cell-surface protein induced in keratinocytes during mouse skin carcinogenesis (Gandarillas *et al*., 1997), we analyzed CD44 and podoplanin expression in cell lines and tumors corresponding to different stages of carcinogenesis (Figure 1, C and D). In both cases, the coordinated up-regulation of podoplanin and CD44s was associated with the undifferentiated phenotype. CD44s was barely detected in the normal epidermis and in benign papillomas, but it was clearly induced in SCCs and further increased in poorly differentiated tumors (Figure 1C). We, therefore, observed an overall increase in CD44 expression that correlated with malignant progression during carcinogenesis in vivo. Furthermore, epithelial premalignant (MCA3D and PB) and weakly metastatic carcinoma (PDV and B9) cell lines expressed low or null amounts of CD44s (Figure 1D); however, its expression was significantly enhanced in highly invasive carcinoma cell lines exhibiting a fibroblastic or spindle phenotype (HaCa4, A5, CarC, and CarB), and this increase occurred concomitantly to down-regulation of CD44v. For a summary of characteristics of the epidermal cell lines used in this study, see Table S1 in supplemental material. Interestingly, podoplanin expression followed a pattern roughly similar to that of CD44s in tumors and cell lines (Figure 1, C and D). The pair of cell lines B9 and A5 representing a homogeneous model for malignant progression is illuminating in this respect. Both cell lines were derived from the same carcinoma, B9 from the squamous component and A5 from the anaplastic spindle region (Burns *et al*., 1991). While B9 neither expressed CD44s nor podoplanin, both glycoproteins were present in A5 cells (Figure 1D). Furthermore, the ectopic expression of mouse podoplanin in pre-malignant MCA3D keratinocytes promoted an EMT associated with the acquisition of highly invasive and metastatic properties (Scholl *et al*., 1999; Scholl *et al*., 2000) and the induction of CD44s expression (Figure 1D). Both podoplanin and CD44s protein levels were also increased in LN11 cells derived from a lymph node metastasis produced by podoplanin-expressing MCA3D cells (Figure 1D and Table S1).

Podoplanin Interacts with CD44s

The subcellular localization of CD44 in podoplanin-expressing cells was analyzed by confocal microscopy. Images revealed that CD44 was distributed along the plasma membrane, concentrated at cell surface protrusions where it colocalized with podoplanin. This was the case for MDCK cells expressing exogenous podoplanin tagged with eGFP (P_{WT} eGFP) and oral carcinoma HN5 cells expressing endogenous podoplanin (Figure 2A). To determine whether the binding of HA to CD44 affected the membrane localization of podoplanin, P_{WT} eGFP cells plated onto coverslips were incubated with 5-μm beads coated with HA. As shown in Figure 2B, podoplanin was recruited by HA-coated beads together with CD44. Binding was specific, as control BSA-coated beads did not trigger recruitment of CD44 or podoplanin. To analyze the possibility of a physical association between podoplanin and CD44, we performed coclustering experiments in P_{WT} eGFP-expressing HN5 cells. These cells were treated in vivo with an antibody raised to the CD44 ectodomain (HP2/9), and then the antibody was clustered with a secondary antibody. This resulted in the formation of

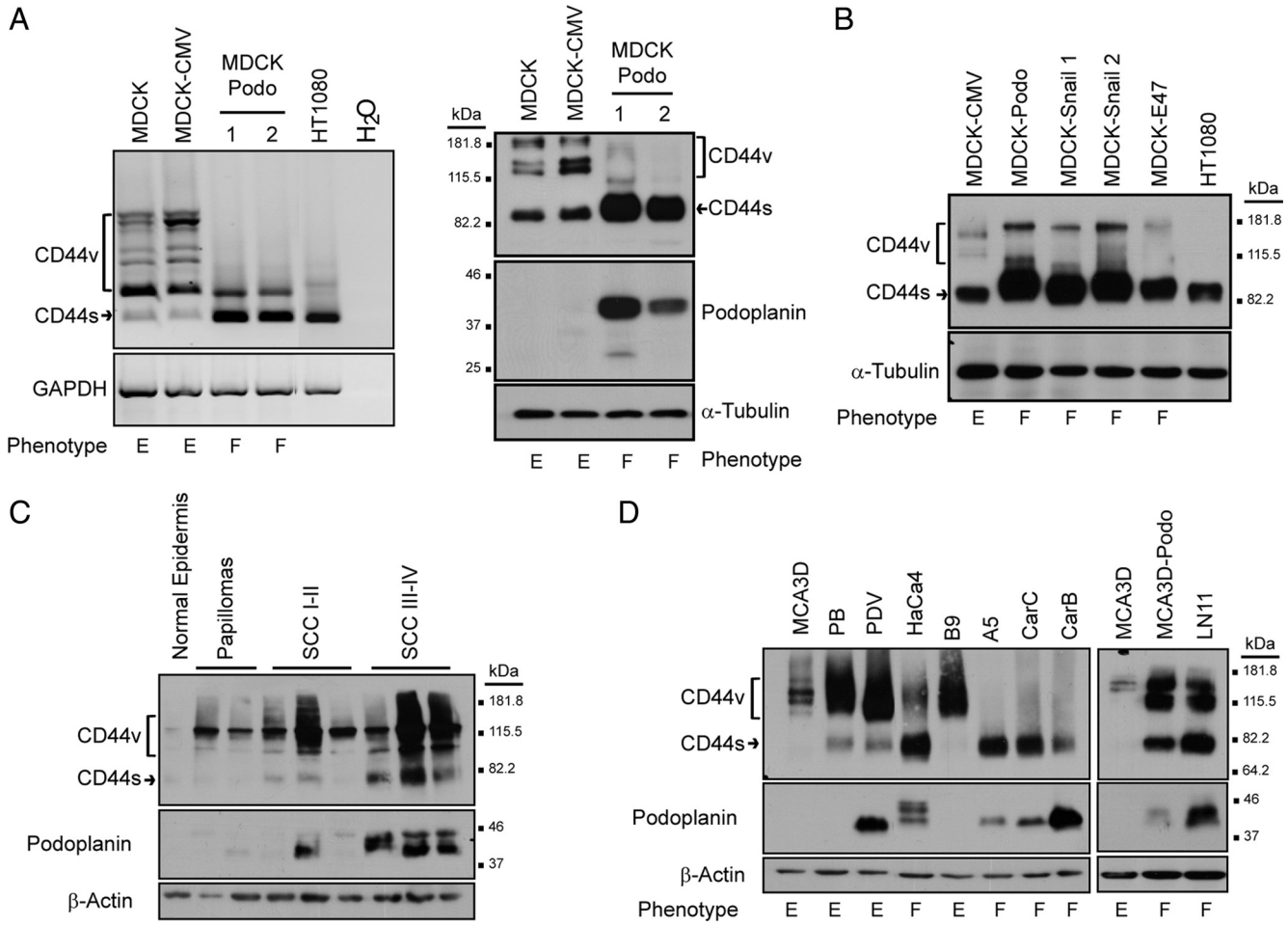

Figure 1. Podoplanin and CD44 expression during EMT and mouse skin carcinogenesis. (A) Podoplanin-promoted EMT in MDCK cells is associated with induction of CD44s expression. The phenotype of the cell lines is indicated: E, epithelial; F, fibroblastic. The morphology and characterization of these cells is shown in Supplemental Figure S1 and in Martin-Villar *et al*. (2006). The fibrosarcoma HT1080 cell line was used as a positive control for CD44s expression. Left and right panels show, respectively, the expression of CD44 transcripts (RT-PCR) and proteins (Western blot). (B) CD44 protein expression in MDCK cells that underwent EMT by transfection of E-cadherin repressors Snail 1, 2, and E47. (C) CD44 and podoplanin protein expression in mouse normal epidermis and skin tumors induced by two-stage carcinogenesis. All squamous cell carcinomas (SCCs) were excised at 43 wk post-initiation. SCCI-II, well to moderately differentiated; SCCIII-IV, poorly differentiated. (D) CD44 and podoplanin protein expression in mouse epidermal cell lines (see table S1 for further information of the cells lines). MCA3D keratinocytes forced to express podoplanin (MCA3D-Podo) undergo EMT. CD44s, CD44 standard isoform; CD44v, variant CD44 isoforms. GAPDH and α-tubulin/β-actin were used as loading controls for RNA and protein, respectively.

CD44 fluorescent spots on the cell surface and in cell–cell contacts (Figure 2C). Interestingly, CD44 clustering induced corecruitment of P_{WT}eGFP suggesting that both proteins are associated either directly or indirectly within the plasma membrane. Reciprocally, clustering of podoplanin also induced corecruitment of CD44 (Figure S2).

We next studied the interaction of these proteins by coimmunoprecipitation analysis. To this end, HEK293T cells were cotransfected with constructs encoding podoplanin and CD44s tagged with Flag and hemagglutinin (Hae) epitopes at the COOH-terminal end, respectively (see in Figure 5A a schematic representation of these constructs). Expression of both molecules resulted to be heterogeneous in their apparent molecular masses as several bands were detected in the immunoblots (Figure 3 and Supplemental Figure S3). We have previously shown that podoplanin heterogeneity in SDS-PAGE arises from the presence of O-linked carbohydrates in its ectodomain (Scholl *et al*., 1999; Martin-Villar *et al*., 2005). Similarly, molecular mass variability of CD44s has been commonly attributed to glycosylation changes, in particular N-linked oligosaccharides (Camp *et al*., 1991; Skelton *et al*., 1998). Indeed, removal of N-linked sugars in the CD44s protein confirmed that extracellular modifications were largely responsible for CD44s molecular mass heterogeneity (Supplemental Figure S3, C and D). Immunoprecipitation experiments confirmed that CD44 and podoplanin coprecipitated with each other (Figure 3A). Interestingly, coprecipitated CD44s and podoplanin had a lower molecular mass (45–65 kDa for CD44s, and ~30 kDa for podoplanin; Figure 3A and Supplemental Figure S3) than that of the corresponding mature fully glycosylated forms, indicating that the interaction between podoplanin and CD44s could be dependent on the carbohydrate structure present in the extracellular domain of both molecules. To confirm these results in a different cellular system, we also performed immunoprecipitation assays using the SCC cell line CarC, because it expresses high levels of podoplanin and CD44s (Figure 1D). The occurrence of endogenous partially glycosylated forms of both podoplanin (~30 kDa) and CD44s (~70 kDa) was confirmed in CarC lysates (Figure 3B).

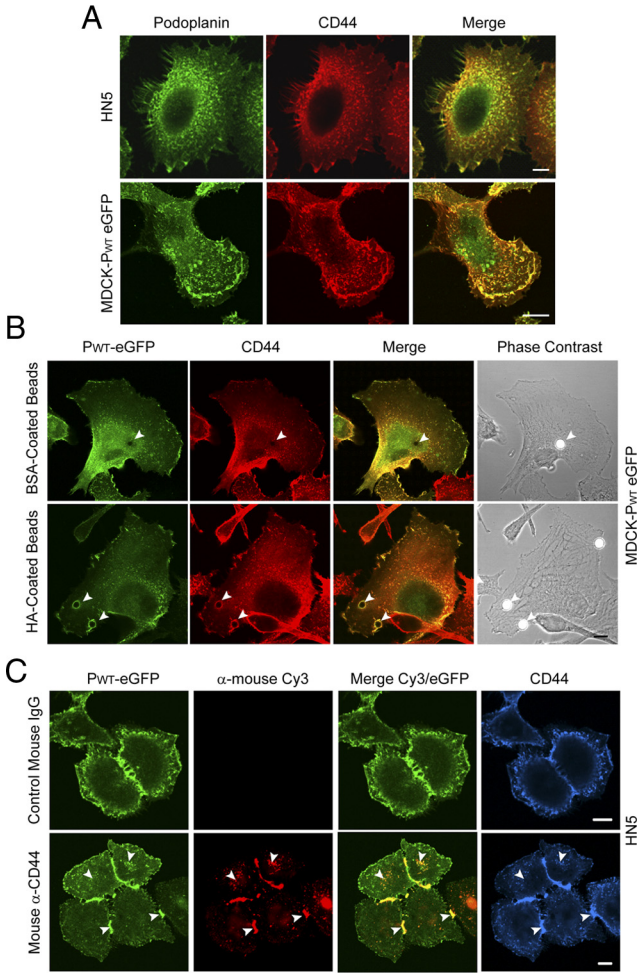

Figure 2. Podoplanin and CD44 colocalize at cell-surface protrusions. (A) Confocal microscopy showing localization of endogenous podoplanin and CD44 in HN5 oral carcinoma cells, and in MDCK cells stably transfected with podoplanin-eGFP (P_{WT} eGFP). (B) Recruitment of both podoplanin and CD44 by HA-coated beads (arrowheads). MDCK-P_{WT} eGFP cells plated onto coverslips were incubated with 5-μm beads coated with BSA or HA for 15 min. Cells were then processed for immunofluorescence to detect CD44. (C) Ab-induced clustering of CD44 (HP2/9 mAb, red) induced corecruitment of P_{WT} GFP (green) to CD44 patches (arrowheads) in HN5 cells. CD44 staining (blue) was performed using a different CD44 mAb (IM7) to visualize total distribution of CD44. Mouse IgGs were used as a negative control. Bars, 10 μm.

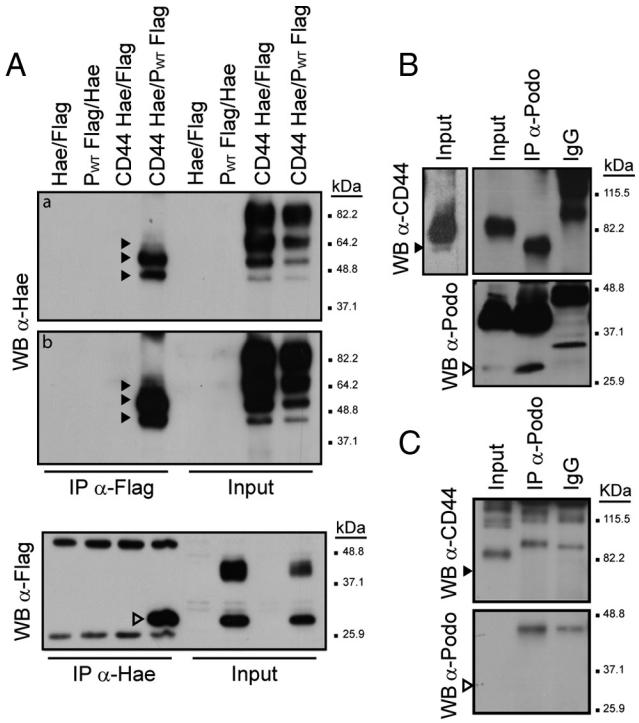

Figure 3. Podoplanin coimmunoprecipitates with CD44s. (A) HEK293T were transiently cotransfected with Flag-tagged human podoplanin or Hae-tagged human CD44s, as indicated. After 24 h of transfection, total lysates were immunoprecipitated with anti-Hae or anti-Flag Abs. Immunoprecipitates were electrophoresed by 10% SDS-PAGE and immunoblotted with anti-Flag or anti-Hae Abs, respectively. Panels a and b represent different exposure times of the same immunoblot. (B) Coimmunoprecipitation of endogenous CD44 and podoplanin in the mouse carcinoma cell line CarC. Lysates were immunoprecipitated with either a mAb specific for mouse podoplanin (PA2.26) or rat IgG as a control. The presence of podoplanin and CD44s in the precipitate was determined with anti-podoplanin PA2.26 and anti-CD44 IM7 mAbs, respectively. A longer exposure time of the input showing the occurrence of a ~70 kDa CD44s form in CarC lysates is shown in the left panel. (C) Coimmunoprecipitation assay in HaCaT keratinocytes. Note that HaCaT cells do not express podoplanin and were used as negative control for the coimmunoprecipitation assays depicted in panel B. Arrowheads indicate incompletely glycosylated forms of CD44s (black arrowheads) and podoplanin (open arrowheads).

Interestingly, endogenous ~70 kDa CD44s was coprecipitaed with a specific Ab recognizing murine podoplanin (PA2.26 mAb). These results demonstrate that podoplanin interacts with CD44s in SCC cells.

Podoplanin Binds CD44s at Cell-Surface Protrusions

The interaction of podoplanin with CD44s on the plasma membrane of MDCK cells was also confirmed in vivo by fluorescence resonance energy transfer (FRET) monitored by the acceptor photobleaching method. The mean FRET efficiency value (n = 8) between eYFP-tagged podoplanin (acceptor) and eCFP-tagged CD44s (donor) was 16% (Figure S4). To further analyze the spatial relationship between podoplanin and CD44s in vivo we used fluorescence lifetime imaging microscopy (FLIM) to monitor FRET. This technique enables visualization and quantification of protein–protein interactions by analysis of the donor lifetime decay kinetics (Parsons *et al.*, 2008). Interaction of P_{WT} eGFP (donor) and CD44s-mRFP (acceptor) was observed in single polarized cells, as measured by decreases in eGFP donor fluorescence lifetime relative to its lifetime in control cells expressing P_{WT} eGFP alone (Figure 4B, compare with panel A). FRET was localized at the trailing edge during rear retraction, and on small foci that were distributed throughout the apical surface of the cell across the lamellae. Interestingly, FRET efficiency was significantly decreased in cells in contact. Although specific interaction in the free lamellas at the outer edge of the colonies was sometimes detected, no interaction was observed at cell junctions, despite the presence of high levels of both molecules (Figure 4, B and C). Moreover, stimulation of MDCK cell migration/scattering with EGF or HGF increased the number of cells in which podoplanin–CD44s complexes were present (data not shown).

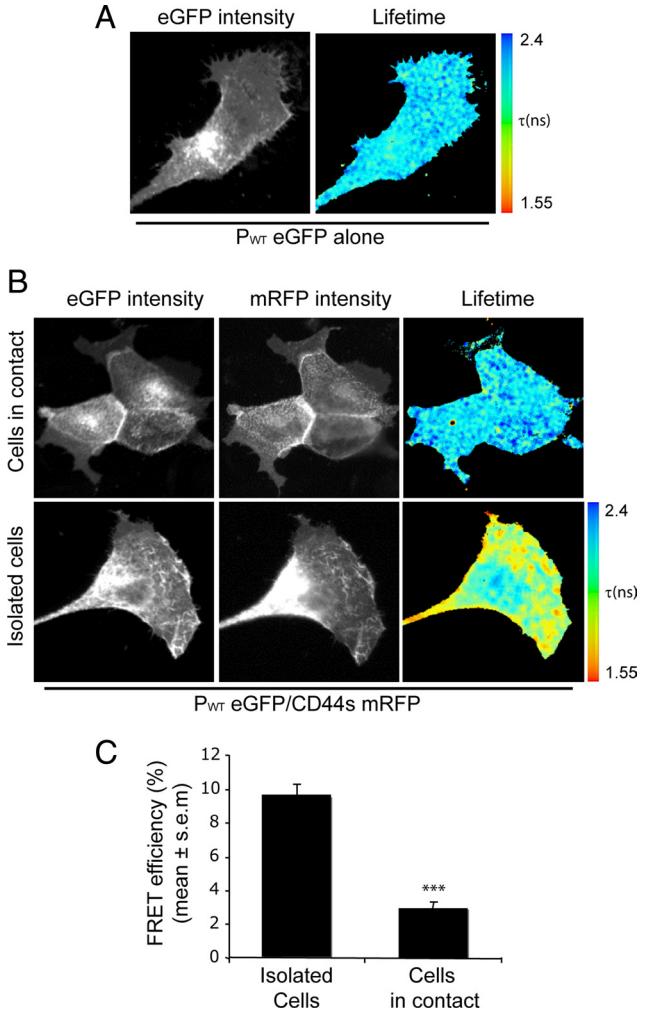

Figure 4. Podoplanin–CD44s complexes at the plasma membrane are up-regulated in cells with a migratory phenotype. (A–C) Multiphoton FLIM was used to image FRET between P_{WT} eGFP (donor) and CD44s-mRFP (acceptor) in MDCK cells. The images show the eGFP multiphoton intensity image and (where appropriate) the corresponding wide-field CCD camera image of mRFP expression. Lifetime images mapping spatial FRET across the cells are depicted using a pseudocolor scale (blue, normal eGFP lifetime; red, FRET). (A) Control MDCK cells expressing P_{WT} eGFP alone demonstrated a normal GFP lifetime (τ in ns) in the absence of acceptor. (B) Cells coexpressing P_{WT} eGFP and CD44s-mRFP display a localized shortening of the eGFP fluorescence lifetime, which is demonstrated by red in the pseudocolor scale. Note that although colocalization between P_{WT} eGFP and CD44s–mRFP was always detected, FRET was recorded mainly in isolated cells (i.e., those that had detached from their neighbors). (C) Bar graph representing average FRET efficiency of 14 cells for each condition over three independent experiments. The Student's *t* test was used to evaluate statistical significance between different populations of data. ***$p < 0.0005$.

These results strongly suggest that podoplanin–CD44s interaction may contribute to a motile phenotype.

Podoplanin Binding to CD44s Is not Mediated by ERM Proteins

The fact that podoplanin–CD44s interaction could be monitored by FRET suggested that the molecules may interact directly. However, because both CD44 and podoplanin bind to ERM proteins through their cytoplasmic (CT) tails, we also investigated the possibility that their interaction could be mediated by ERM proteins. To analyze this, podoplanin mutant constructs lacking the CT tail ($P_{\Delta CT}$) or the ERM binding site (P_{QNN}) were used for FRET/FLIM experiments (Figure 5A). As depicted in Figure 5B-C, preventing the binding of ezrin/moesin to podoplanin (Martin-Villar *et al.*, 2006) did not impair CD44s–podoplanin interaction, indicating that it is not mediated by ERM proteins. To further analyze which regions of the podoplanin molecule are important for podoplanin–CD44s binding we carried out coimmunoprecipitation experiments in HEK293T cells. These experiments were performed coexpressing CD44s-Hae and several podoplanin mutant constructs fused to eGFP, including $P_{\Delta CT}$, P_{QNN} and a mutant construct lacking the extracellular domain ($P_{\Delta EC}$). All these mutant proteins have been previously characterized (Martin-Villar *et al.*, 2006). The ability of $P_{\Delta EC}$ mutant to interact with CD44s in vivo could not be tested in FRET/FLIM experiments due to the fact that the eGFP tag in this construct is located at the NH_2-terminal end of the fusion protein (Figure 5A). However, coimmunoprecipitation assays showed that only the deletion of the podoplanin extracellular domain prevented its interaction with CD44s (Figure 5D) confirming that ERM proteins are not required for podoplanin–CD44s (figure 5D) association. Likewise, these results indicate that the podoplanin ectodomain is a crucial region for its binding to CD44.

Podoplanin-Induced Cell Migration and Directionality Requires CD44

To analyze the contribution of CD44 to podoplanin-induced cell migration, we performed transwell assays using MDCK cells transiently cotransfected with podoplanin cDNA and a small interfering (si)RNA to mediate down-regulation of CD44. Confirming our previous findings (Martin-Villar *et al.*, 2006), P_{WT} eGFP expression increased MDCK cell migration ~1.7-fold (Figure 6). The knockdown of CD44 (~70% reduction) did not significantly change the migratory behavior of MDCK-eGFP cells. However, CD44 down-regulation prevented podoplanin-enhanced migration, demonstrating that podoplanin requires CD44 to promote cell migration in MDCK cells (Figure 6, A and B).

Our previous observations suggested that podoplanin promotes intrinsic directional motility in MDCK cells (Martin-Villar *et al.*, 2006). To further investigate this, MDCK cells were imaged by fluorescence time-lapse microscopy allowing measurement of the total distance traveled, the displacement from origin, and calculation of mean speed and directional persistence (Figure 6, C and D). The migration pattern of control MDCK cells was erratic, with cells often changing direction, while P_{WT} eGFP-expressing cells frequently continued migrating in the same direction without turning. Comparison of the migration tracks of a representative number of cells for each condition showed that the directionality ratio was significantly increased in podoplanin-expressing cells, and that this was prevented when CD44 was knocked-down. Neither podoplanin expression nor CD44 down-regulation affected the migration speed of MDCK cells (Figure 6, C and D). Altogether, these results demonstrate that CD44 plays a crucial role in podoplanin-mediated migration.

Podoplanin and CD44 Depletion Alters Lamellipodia Extension/Stabilization and Cell Spreading

To further analyze the role of the podoplanin–CD44 complex in the migration of tumor cells, we down-regulated the

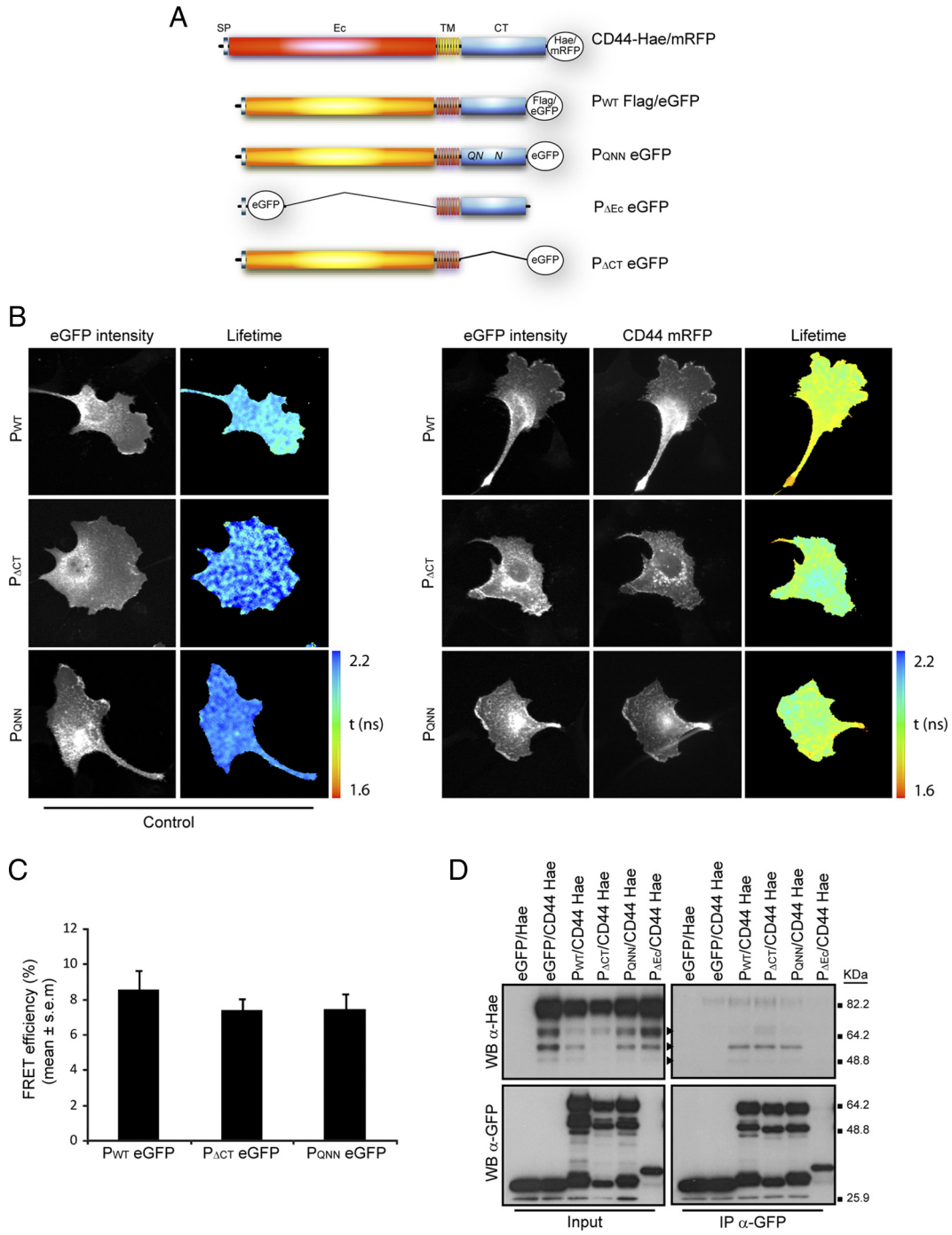

Figure 5. Podoplanin–CD44s interaction is not mediated by ERM proteins. (A) Schematic representation of podoplanin and CD44s fusion constructs used for coimmunoprecipitation and FRET/FLIM assays. SP, signal peptide; Ec, ectodomain; TM, transmembrane domain; CT, cytoplasmic tail; QN N, positive charged residues (RK.R) in podoplanin juxtamembrane domain were substituted by uncharged polar amino acids (QN.N) in order to impair podoplanin binding to ERM proteins (Martin-Villar *et al.*, 2006). (B) MDCK cells were cotransfected with CD44s mRFP and podoplanin eGFP mutant constructs, and cells were then imaged by FLIM to detect FRET as depicted in Figure 4. Images show the eGFP multiphoton intensity image and (where appropriate) the corresponding wide-field CCD camera image of the mRFP expression. Control MDCK cells expressing P_{WT}, $P_{\Delta CT}$, or P_{QNN} eGFP alone showed a normal GFP lifetime (τ in ns) in the absence of acceptor (CD44s mRFP), while cells coexpressing CD44s mRFP and podoplanin mutant constructs displayed a localized shortening of the eGFP fluorescence lifetime. (C) The bar graph represents average FRET efficiency of 15 cells over three independent experiments. (D) Coimmunoprecipitation assays performed in HEK293T cells coexpressing CD44s Hae and podoplanin eGFP mutant constructs. Total cell lysates were immunoprecipitated with an anti-GFP Ab-conjugated resin as described in Materials and Methods. The coimmunoprecipitated products were detected with an anti-Hae Ab.

expression of both molecules in the SCC cell line HN5, which expresses high levels of endogenous podoplanin and CD44. We used a vector-based small hairpin (sh)RNA approach to deplete podoplanin, in combination with an al-

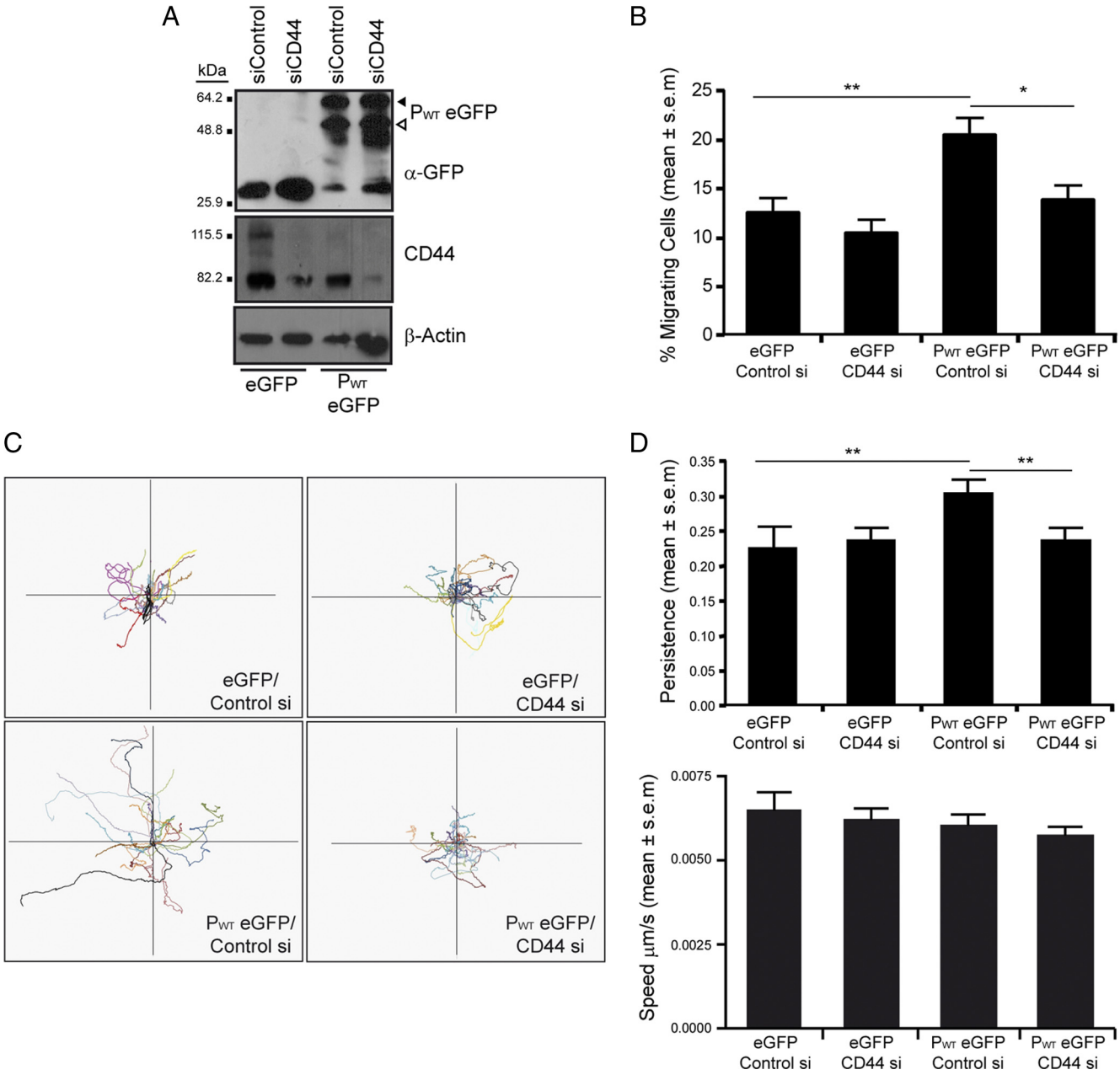

Figure 6. Podoplanin-induced migration and directionality in MDCK cells requires CD44. (A) Expression levels of podoplanin (P_{WT} eGFP) and CD44 after P_{WT} eGFP and CD44 siRNA coexpression. β-actin was used as a loading control. Arrowheads indicate fully (black arrowheads) and incompletely glycosylated (open arrowheads) forms of PWT eGFP. (B) Transwell migration assay. Bar graph representing percentage of migrating cells per total number of cells. Results are representative of three independent experiments performed in duplicates. (C) Representative migration tracks of MDCK cells expressing P_{WT} eGFP in the presence or absence of CD44 (n = 30). (D) Average persistence and speed of migration derived from the tracks depicted in C. n = 40–85 cells per bar. Asterisks indicate significant differences in a Student's t test. **$p < 0.005$, *$p < 0.05$.

ready established siRNA to mediate the knockdown CD44 in human cells (Tzircotis *et al.*, 2005). As depicted in Figure 7A, CD44 expression was efficiently down-regulated (~70%), and similarly, podoplanin protein levels were almost completely suppressed (~90% reduction) by using two different shRNAs (podo-sh1 and -sh2). A significant siRNA-mediated reduction of CD44 levels (~80%) was also achieved in podoplanin-depleted cells. siRNA mediated down-regulation of CD44 seemed not to affect podoplanin expression and vice versa.

Control cells usually displayed a characteristic highly organized leading edge with well-extended lamellipodia extensions, and the microtubule network often aligned parallel to, but localized at a considerable distance from, the leading edge. Interestingly, the single knockdown of CD44 enhanced cell spreading whereas the opposite was found to occur by silencing podoplanin expression alone (Figure 7, B and C). CD44si cells extended wide lamella with clear marginal F-actin ruffles. These cells also showed a well organized microtubule network (Figure 7B). Podoplanin-deficient cells,

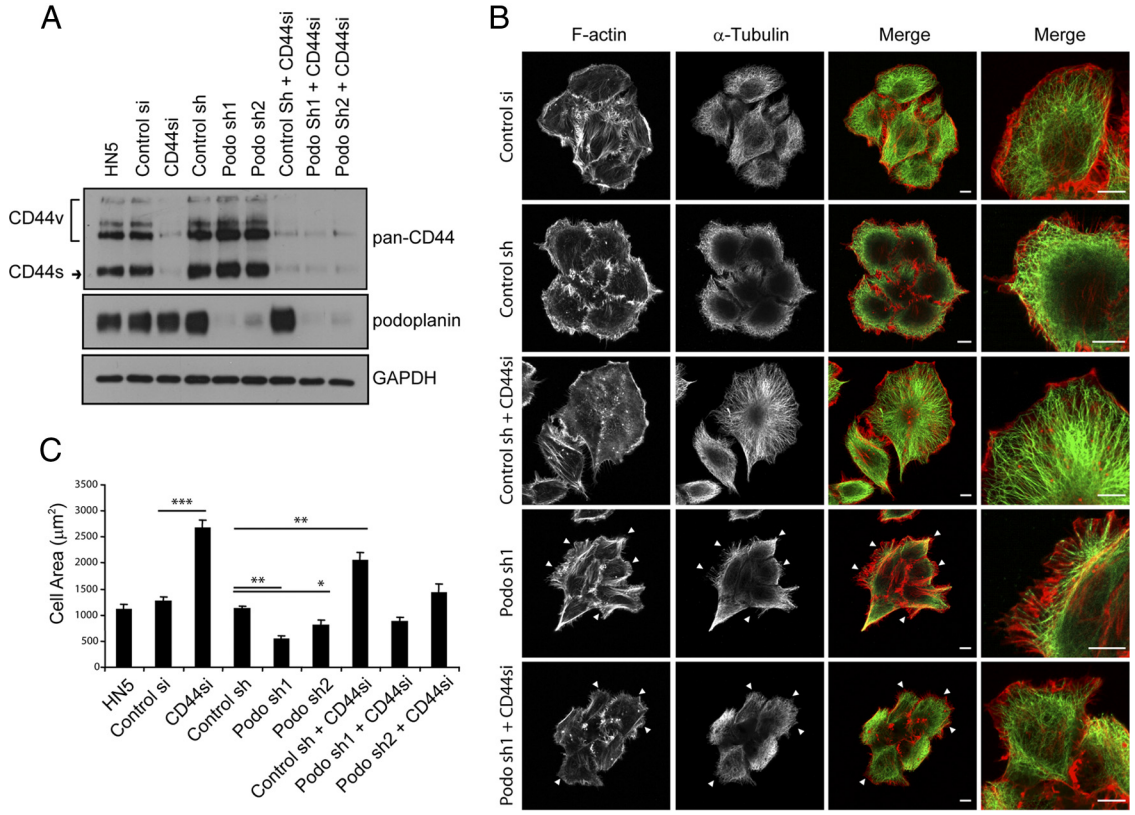

Figure 7. Knockdown of CD44 and podoplanin in oral carcinoma HN5 cells affects cell spreading. (A) Expression levels of CD44 and podoplanin in single and double knockdown cells by Western blot analysis. The expression of GAPDH was used as a loading control. (B) Immunofluorescence detection of F-actin and microtubules in single and double knockdown cells. Cells were double stained for F-actin (red) with phalloidin and microtubules (green) with a specific anti-tubulin mAb. Note the extremely disorganized leading edge of podoplanin-deficient cells and double knockdown cells (arrowheads) compared with control cells. (C) Graphical representation of the cell spread areas quantified using Image J software as described in Materials and Methods (n = 40–50 cells per bar). P values were obtained using a one-way analysis of variance (ANOVA). *$p < 0.05$; **$p < 0.005$; ***$p < 0.0005$. Bars, 10 μm.

however, had an extremely disorganized leading edge. These cells were unable to extend typical broad lamellipodia, exhibiting narrower (filopodia-like) protrusions instead, and the microtubules penetrated into the leading edge area (Figure 7B). RNAi-mediated knockdown of endogenous CD44 in podoplanin-deficient cells did not significantly change the cell shape of these cells (Figure 7, B and C). These results point to a role of the podoplanin–CD44 complex in regulating lamellipodia extension/stabilization during cell spreading and migration.

Podoplanin and CD44 Cooperate to Promote Directional Cell Motility during Wound Healing

To assess whether the observed morphological changes in single and double knockdown HN5 cells were coupled with defects in cell motility, we performed an in vitro wound healing assay. Time-lapse video microscopy was used to monitor wound closure. All the control cell lines showed ~95% wound closure 18 h after wounding. Podo-sh1 and sh2 cells covered ~40 and 60% of the control area, respectively, and CD44si cells covered 20–30% in the same period of time. Interestingly, wound closure delay became significantly more evident in double knockdown cells, as only 2–10% of the wound area was covered (Figure 8B and Movie 1 in supplemental material). Subsequently, we analyzed the migration pattern of a representative number of cells at the wound edges for a time period of 6 h. When the migration tracks were graphed to show directionality, it was evident that down-regulation of either podoplanin or CD44 alone resulted in a more random, less directional movement of cells positioned along the wound edge (Figure 8, A and C and Movie 2 in supplemental material). Moreover, by silencing both molecules the migration of HN5 cells toward the wound was almost suppressed. Altogether, these results strongly indicate that podoplanin and CD44 collaborate to promote directional motility.

DISCUSSION

Podoplanin and CD44 are type I membrane glycoproteins that are anchored to the actin cytoskeleton through association with ERM proteins (Legg and Isacke, 1998; Yonemura *et al*., 1998; Scholl *et al*., 1999; Martin-Villar *et al*., 2006), and both are involved in cell adhesion, motility, and signal transduction despite lacking intrinsic kinase activity (reviewed in Ponta *et al*., 2003; Wicki and Christofori, 2007). In this study, we report CD44 as a novel binding partner for podoplanin and describe a close relationship between CD44s and podoplanin expression associated with EMT and advanced stages of tumor progression in an experimental model of carcinogenesis. Although studies regarding expression of CD44 isoforms in human cancer are contradictory (Marhaba and Zoller, 2004), it has been proposed that a switch from CD44v to CD44s expression is a feature of poorly differentiated

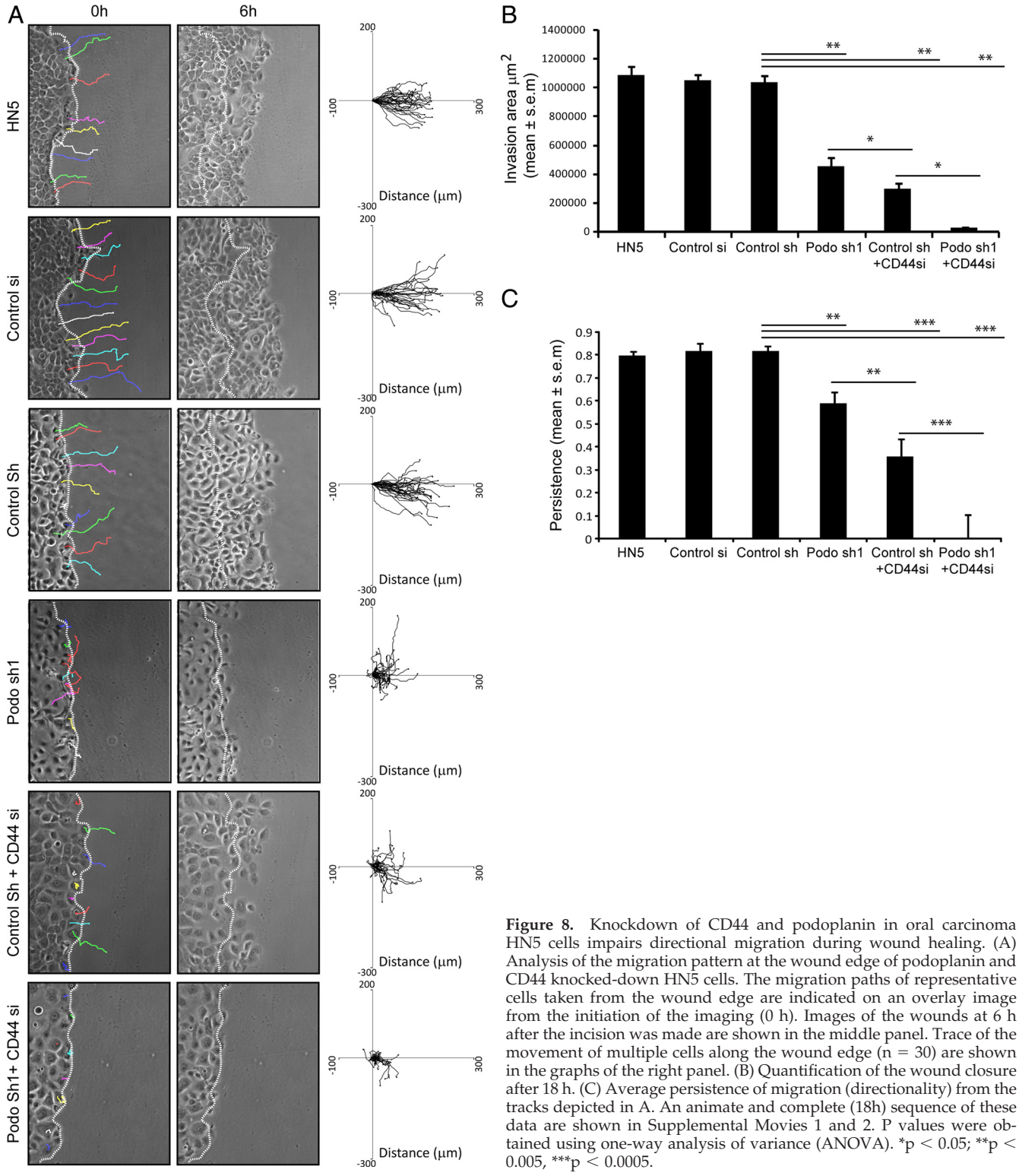

Figure 8. Knockdown of CD44 and podoplanin in oral carcinoma HN5 cells impairs directional migration during wound healing. (A) Analysis of the migration pattern at the wound edge of podoplanin and CD44 knocked-down HN5 cells. The migration paths of representative cells taken from the wound edge are indicated on an overlay image from the initiation of the imaging (0 h). Images of the wounds at 6 h after the incision was made are shown in the middle panel. Trace of the movement of multiple cells along the wound edge (n = 30) are shown in the graphs of the right panel. (B) Quantification of the wound closure after 18 h. (C) Average persistence of migration (directionality) from the tracks depicted in A. An animate and complete (18h) sequence of these data are shown in Supplemental Movies 1 and 2. P values were obtained using one-way analysis of variance (ANOVA). *$p < 0.05$; **$p < 0.005$, ***$p < 0.0005$.

SCCs (Hudson *et al*., 1996; Stoll *et al*., 1999). Accordingly, our conclusion from the analysis of both tumors and cell lines derived from the mouse skin carcinogenesis model is that despite the high heterogeneity of CD44 expression in vivo, a clear CD44s (and podoplanin) up-regulation is observed associated with the loss of differentiation in skin carcinomas. Similarly, increased expression of podoplanin has been associated with poor clinical outcome and metastasis in human SCCs (Yuan *et al*., 2006; Chuang *et al*., 2009). Interestingly, a recent study has found that podoplanin and CD44 were coexpressed in cells localized at the periphery of tumor nests in a high proportion of SCCs of the lung, although the distribution of CD44 was broader than that of podoplanin (Shimada *et al*., 2009). Moreover, CD44 is a common cell-

surface marker for cancer stem cells in solid tumors (Visvader and Lindeman, 2008), and podoplanin has recently been postulated as a novel candidate marker of SCC stem cells, where it was coexpressed with CD44 (Atsumi *et al*., 2008). These data suggest that there is a subpopulation of carcinoma cells with stem-like properties that coexpress podoplanin and CD44. While the biological significance of the presence of both proteins in cancer stem cells is still uncertain, it is tempting to speculate that coexpression of podoplanin and CD44s identify a cancer stem cell subpopulation with a high potential to disseminate and metastasize because of its association with EMT and the undifferentiated state of SCCs (Polyak and Weinberg, 2009).

Interestingly, we also found that podoplanin and CD44s interact to form a dynamic complex at the plasma membrane of migratory cells. This interaction seems to be direct, as it is not mediated by their common partners ezrin/moesin, and might be dependent on extracellular modifications of both glycoproteins. Supporting this hypothesis is the finding that the extracellular domain of podoplanin appears to be crucial for its association with CD44s. Accordingly, podoplanin interactions with other proteins such as CLEC-2 (Kato *et al*., 2008) or galectin-8 (Cueni and Detmar, 2009) have been found to be dependent on the carbohydrate moieties present in their ectodomains. Moreover, it has been recently reported that recombinant soluble forms of the podoplanin ectodomain with different degrees of glycosylation can decrease cell adhesion and migration of lymphatic endothelial cells. Interestingly, in this study, the less glycosylated forms were more effective than the more extensively glycosylated proteins (Cueni *et al*., 2010). CD44 is known to undergo sequential proteolytic cleavages that have an important role in cell migration (reviewed in Nagano and Saya, 2004). For this reason, one could argue that the CD44 forms (~45–70 kDa) coprecipitating with podoplanin might be fragments of the molecule rather than less glycosylated proteins. However, these forms were recognized either by antibodies raised to the CD44 NH_2-terminal end (IM7: Figure 3B) or to its CT tail (anti-CD44cyto Ab or anti-Hae Ab; Figure 3A and Supplemental Figure S3), indicating that these forms are not processing products of 80-kDa CD44s. Moreover, inhibition of CD44 proteolysis did not alter the pattern of CD44s coprecipitating forms (Supplemental Figure S3). On the other hand, removal of N-linked oligosaccharides in the CD44s molecule gave rise to protein forms of ~45–70 kDa with similar apparent molecular masses as the ones precipitated together with podoplanin. Glycosylation has been implicated in the regulation of CD44-mediated cell binding to HA, as well as in CD44 association with the actin cytoskeleton (Thorne *et al*., 2004). The fact that podoplanin–CD44s interaction preferentially occurs when both molecules are not heavily glycosylated allows us to speculate that this association could be regulated by the glycosylation status of both molecules. Further investigations to address the mechanisms that regulate podoplanin–CD44s complex formation and its dependence on differential glycosylation are currently in progress.

Podoplanin–CD44s interaction appears to occur mainly on the trailing edge and on discrete foci on the lamella. Because both proteins can activate RhoA GTPase through binding to ERM proteins (Hirao *et al*., 1996; Martin-Villar *et al*., 2006), and RhoA-ROCK activity is required for actomyosin-based cortical contractility leading to detachment of the trailing edge (Ridley, 2001), podoplanin–CD44s interaction might be associated with tail retraction during mesenchymal-type of tumor cell movement (Friedl and Wolf, 2003). However, it is not clear yet how binding of these molecules to ERM proteins affects podoplanin–CD44s association and whether podoplanin–CD44s interaction influences signal transduction pathways mediated by any of these two molecules. On the other hand, knockdown of CD44 in HN5 oral SCC cells resulted in increased spreading and formation of extended lamella, while the opposite effect was observed upon silencing podoplanin expression. Moreover, knockdown of CD44 in podoplanin-deficient cells did not change significantly the shrunken shape characteristic of these cells. These results also suggest an involvement of podoplanin in lamellipodial extension/stabilization and spreading that is regulated by CD44. What strongly emerges from our gain- and loss-of-function experiments is the notion that podoplanin and CD44 cooperate to stimulate directional motility. Thus, podoplanin enhances the intrinsic directional motility of MDCK cells migrating either randomly or in a chemotactic transwell assay, and this effect is abolished by knocking-down CD44. Likewise, single knockdown of either CD44 or podoplanin inhibited the migratory potential of HN5 carcinoma cells in an in vitro wound healing assay, and depletion of both molecules almost suppressed the migration of HN5 cells toward the wound. Both CD44 and podoplanin appear to be required for cells to maintain direction during movement, as the knockdown of any of them resulted in less directional migration. Previous studies have found an important role for CD44 in mediating directional migration of different cell types, including cancer cells (Miletti-Gonzalez *et al*., 2005; Tzircotis *et al*., 2005; Colone *et al*., 2008). Interestingly, in neutrophils and fibroblasts, CD44 is characteristically localized at the trailing edge of polarized cells (Jacobson *et al*., 1984; Seveau *et al*., 2001). It has been found that the binding of CD44 to ezrin is crucial for CD44-dependent directional motility (Legg *et al*., 2002). Also, podoplanin mutant proteins unable to bind ezrin/moesin confer less motile phenotypes than wild-type podoplanin when expressed in MDCK cells (Martin-Villar *et al*., 2006). However, it remains to be investigated whether podoplanin association with ERM proteins controls podoplanin-dependent directional motility as occurs with CD44.

Interest in podoplanin has considerably increased over the years because of its up-regulation in different human tumors, especially those derived from squamous stratified epithelia. However, many aspects of the biology and function of this glycoprotein still remain elusive. The lack of any obvious functional domains in the podoplanin molecule highlights the need to identify its binding partners. Similarly, the precise mechanisms controlling the structural and signaling events associated to CD44 have yet to be elucidated. In summary, the data presented here demonstrate that podoplanin associates with CD44s and that this interaction is important for driving directional cell migration in epithelial and tumor cells. Determining how this interaction is regulated could help to clarify many open questions in the biology of both molecules.

ACKNOWLEDGMENTS

We thank Drs. Amparo Cano, Francisco Sánchez-Madrid, and Helen Yarwood for their generous gifts of cell lines and antibodies and Patricia Carrasco for her help with Western blots. We also thank Dr. Véronique Orian-Rousseau and Helmut Ponta for their technical advice. This work was supported by grant SAF2007-63821 from the Spanish Ministry of Science and Innovation (to M.Q.), the Royal Society University Research Fellowship (to M.P.), Medical Research Council (to G.E.J.) EU FP7 T3Net Consortium (GEJ), and Cancer Research UK (to G.E.J. and E.M.V.).

REFERENCES

Akhurst, R. J., and Balmain, A. (1999). Genetic events and the role of TGF beta in epithelial tumour progression. J. Pathol. *187*, 82–90.

Allen, W. E., Zicha, D., Ridley, A. J., and Jones, G. E. (1998). A role for Cdc42 in macrophage chemotaxis. J. Cell Biol. *141*, 1147–1157.

Atsumi, N., Ishii, G., Kojima, M., Sanada, M., Fujii, S., and Ochiai, A. (2008). Podoplanin, a novel marker of tumor-initiating cells in human squamous cell carcinoma A431. Biochem. Biophys. Res. Commun. *373*, 36–41.

Burns, P. A., Kemp, C. J., Gannon, J. V., Lane, D. P., Bremner, R., and Balmain, A. (1991). Loss of heterozygosity and mutational alterations of the p53 gene in skin tumours of interspecific hybrid mice. Oncogene *6*, 2363–2369.

Camp, R. L., Kraus, T. A., and Pure, E. (1991). Variations in the cytoskeletal interaction and posttranslational modification of the CD44 homing receptor in macrophages. J. Cell Biol. *115*, 1283–1292.

Chuang, W. Y., Yeh, C. J., Wu, Y. C., Chao, Y. K., Liu, Y. H., Tseng, C. K., Chang, H. K., Liu, H. P., and Hsueh, C. (2009). Tumor cell expression of podoplanin correlates with nodal metastasis in esophageal squamous cell carcinoma. Histol. Histopathol. *24*, 1021–1027.

Clark, K., Pankov, R., Travis, M. A., Askari, J. A., Mould, A. P., Craig, S. E., Newham, P., Yamada, K. M., and Humphries, M. J. (2005). A specific alpha5beta1-integrin conformation promotes directional integrin translocation and fibronectin matrix formation. J. Cell Sci. *118*, 291–300.

Colone, M., Calcabrini, A., Toccacieli, L., Bozzuto, G., Stringaro, A., Gentile, M., Cianfriglia, M., Ciervo, A., Caraglia, M., Budillon, A., Meo, G., Arancia, G., and Molinari, A. (2008). The multidrug transporter P-glycoprotein: a mediator of melanoma invasion? J. Invest. Dermatol. *128*, 957–971.

Cueni, L.N., Chen, L., Zhang, H., Marino, D., Huggenberger, R., Alitalo, A., Bianchi, R., and Detmar, M. (2010). Podoplanin-Fc reduces lymphatic vessel formation in vitro and in vivo and causes disseminated intravascular coagulation when transgenically expressed in the skin. Blood. In press.

Cueni, L. N., and Detmar, M. (2009). Galectin-8 interacts with podoplanin and modulates lymphatic endothelial cell functions. Exp. Cell Res. *315*, 1715–1723.

del Pozo, M. A., Alderson, N. B., Kiosses, W. B., Chiang, H. H., Anderson, R. G., and Schwartz, M. A. (2004). Integrins regulate Rac targeting by internalization of membrane domains. Science *303*, 839–842.

Elbashir, S. M., Harborth, J., Lendeckel, W., Yalcin, A., Weber, K., and Tuschl, T. (2001). Duplexes of 21-nucleotide RNAs mediate RNA interference in cultured mammalian cells. Nature *411*, 494–498.

Friedl, P., and Wolf, K. (2003). Tumour-cell invasion and migration: diversity and escape mechanisms. Nat. Rev. Cancer *3*, 362–374.

Gandarillas, A., Scholl, F. G., Benito, N., Gamallo, C., and Quintanilla, M. (1997). Induction of PA2.26, a cell-surface antigen expressed by active fibroblasts, in mouse epidermal keratinocytes during carcinogenesis. Mol. Carcinog. *20*, 10–18.

Hathcock, K. S., Hirano, H., Murakami, S., and Hodes, R. J. (1993). CD44 expression on activated B cells. Differential capacity for CD44-dependent binding to hyaluronic acid. J. Immunol. *151*, 6712–6722.

Hirao, M., Sato, N., Kondo, T., Yonemura, S., Monden, M., Sasaki, T., Takai, Y., and Tsukita, S. (1996). Regulation mechanism of ERM (ezrin/radixin/moesin) protein/plasma membrane association: possible involvement of phosphatidylinositol turnover and Rho-dependent signaling pathway. J. Cell Biol. *135*, 37–51.

Hudson, D. L., Speight, P. M., and Watt, F. M. (1996). Altered expression of CD44 isoforms in squamous-cell carcinomas and cell lines derived from them. Int. J. Cancer *66*, 457–463.

Isacke, C. M., and Yarwood, H. (2002). The hyaluronan receptor, CD44. Int. J. Biochem. Cell Biol. *34*, 718–721.

Jacobson, K., O'Dell, D., Holifield, B., Murphy, T. L., and August, J. T. (1984). Redistribution of a major cell surface glycoprotein during cell movement. J. Cell Biol. *99*, 1613–1623.

Kato, Y., Kaneko, M. K., Kunita, A., Ito, H., Kameyama, A., Ogasawara, S., Matsuura, N., Hasegawa, Y., Suzuki-Inoue, K., Inoue, O., Ozaki, Y., and Narimatsu, H. (2008). Molecular analysis of the pathophysiological binding of the platelet aggregation-inducing factor podoplanin to the C-type lectin-like receptor CLEC-2. Cancer Sci. *99*, 54–61.

Kunita, A., Kashima, T. G., Morishita, Y., Fukayama, M., Kato, Y., Tsuruo, T., and Fujita, N. (2007). The platelet aggregation-inducing factor aggrus/podoplanin promotes pulmonary metastasis. Am. J. Pathol. *170*, 1337–1347.

Legg, J. W., and Isacke, C. M. (1998). Identification and functional analysis of the ezrin-binding site in the hyaluronan receptor, CD44. Curr. Biol. *8*, 705–708.

Legg, J. W., Lewis, C. A., Parsons, M., Ng, T., and Isacke, C. M. (2002). A novel PKC-regulated mechanism controls CD44 ezrin association and directional cell motility. Nat. Cell Biol. *4*, 399–407.

Marhaba, R., and Zoller, M. (2004). CD44 in cancer progression: adhesion, migration and growth regulation. J. Mol. Histol. *35*, 211–231.

Martin-Villar, E., Megias, D., Castel, S., Yurrita, M. M., Vilaro, S., and Quintanilla, M. (2006). Podoplanin binds ERM proteins to activate RhoA and promote epithelial-mesenchymal transition. J. Cell Sci. *119*, 4541–4553.

Martin-Villar, E., Scholl, F. G., Gamallo, C., Yurrita, M. M., Munoz-Guerra, M., Cruces, J., and Quintanilla, M. (2005). Characterization of human PA2.26 antigen (T1alpha-2, podoplanin), a small membrane mucin induced in oral squamous cell carcinomas. Int. J. Cancer *113*, 899–910.

Miletti-Gonzalez, K. E., Chen, S., Muthukumaran, N., Saglimbeni, G. N., Wu, X., Yang, J., Apolito, K., Shih, W. J., Hait, W. N., and Rodriguez-Rodriguez, L. (2005). The CD44 receptor interacts with P-glycoprotein to promote cell migration and invasion in cancer. Cancer Res. *65*, 6660–6667.

Nagano, O., and Saya, H. (2004). Mechanism and biological significance of CD44 cleavage. Cancer Sci. *95*, 930–935.

Nakazawa, Y., Sato, S., Naito, M., Kato, Y., Mishima, K., Arai, H., Tsuruo, T., and Fujita, N. (2008). Tetraspanin family member CD9 inhibits Aggrus/podoplanin-induced platelet aggregation and suppresses pulmonary metastasis. Blood *112*, 1730–1739.

Parsons, M., Messent, A. J., Humphries, J. D., Deakin, N. O., and Humphries, M. J. (2008). Quantification of integrin receptor agonism by fluorescence lifetime imaging. J. Cell Sci. *121*, 265–271.

Peinado, H., Olmeda, D., and Cano, A. (2007). Snail, Zeb and bHLH factors in tumour progression: an alliance against the epithelial phenotype? Nat. Rev. Cancer *7*, 415–428.

Perez-Gomez, E., Villa-Morales, M., Santos, J., Fernandez-Piqueras, J., Gamallo, C., Dotor, J., Bernabeu, C., and Quintanilla, M. (2007). A role for endoglin as a suppressor of malignancy during mouse skin carcinogenesis. Cancer Res. *67*, 10268–10277.

Polyak, K., and Weinberg, R. A. (2009). Transitions between epithelial and mesenchymal states: acquisition of malignant and stem cell traits. Nat. Rev. Cancer *9*, 265–273.

Ponta, H., Sherman, L., and Herrlich, P. A. (2003). CD *44*, from adhesion molecules to signalling regulators. Nat. Rev. Mol. Cell Biol. *4*, 33–45.

Quintanilla, M., Ramirez, J. R., Perez-Gomez, E., Romero, D., Velasco, B., Letarte, M., Lopez-Novoa, J. M., and Bernabeu, C. (2003). Expression of the TGF-beta coreceptor endoglin in epidermal keratinocytes and its dual role in multistage mouse skin carcinogenesis. Oncogene *22*, 5976–5985.

Ridley, A. J. (2001). Rho GTPases and cell migration. J. Cell Sci. *114*, 2713–2722.

Roscic-Mrkic, B., Fischer, M., Leemann, C., Manrique, A., Gordon, C. J., Moore, J. P., Proudfoot, A. E., and Trkola, A. (2003). RANTES (CCL5) uses the proteoglycan CD44 as an auxiliary receptor to mediate cellular activation signals and HIV-1 enhancement. Blood *102*, 1169–1177.

Scholl, F. G., Gamallo, C., and Quintanilla, M. (2000). Ectopic expression of PA2.26 antigen in epidermal keratinocytes leads to destabilization of adherens junctions and malignant progression. Lab. Invest. *80*, 1749–1759.

Scholl, F.G., Gamallo, C., Vilaro, S., and Quintanilla, M. (1999). Identification of PA2.26 antigen as a novel cell-surface mucin-type glycoprotein that induces plasma membrane extensions and increased motility in keratinocytes. J. Cell Sci. *112 (Pt* 24), 4601–4613.

Screaton, G. R., Bell, M. V., Jackson, D. G., Cornelis, F. B., Gerth, U., and Bell, J. I. (1992). Genomic structure of DNA encoding the lymphocyte homing receptor CD44 reveals at least 12 alternatively spliced exons. Proc. Natl. Acad. Sci. USA *89*, 12160–12164.

Seveau, S., Eddy, R. J., Maxfield, F. R., and Pierini, L. M. (2001). Cytoskeleton-dependent membrane domain segregation during neutrophil polarization. Mol. Biol. Cell *12*, 3550–3562.

Shimada, Y., Ishii, G., Nagai, K., Atsumi, N., Fujii, S., Yamada, A., Yamane, Y., Hishida, T., Nishimura, M., Yoshida, J., Ikeda, N., and Ochiai, A. (2009). Expression of podoplanin, CD44, and p63 in squamous cell carcinoma of the lung. Cancer Sci. *100*, 2054–2059.

Skelton, T. P., Zeng, C., Nocks, A., and Stamenkovic, I. (1998). Glycosylation provides both stimulatory and inhibitory effects on cell surface and soluble CD44 binding to hyaluronan. J. Cell Biol. *140*, 431–446.

Stoll, C., Baretton, G., Soost, F., Terpe, H. J., Domide, P., and Lohrs, U. (1999). Prognostic importance of the expression of CD44 splice variants in oral squamous cell carcinomas. Oral Oncol. *35*, 484–489.

Thorne, R. F., Legg, J. W., and Isacke, C. M. (2004). The role of the CD44 transmembrane and cytoplasmic domains in co-ordinating adhesive and signalling events. J. Cell Sci. *117*, 373–380.

Tzircotis, G., Thorne, R. F., and Isacke, C. M. (2005). Chemotaxis towards hyaluronan is dependent on CD44 expression and modulated by cell type variation in CD44-hyaluronan binding. J. Cell Sci. *118*, 5119–5128.

Visvader, J. E., and Lindeman, G. J. (2008). Cancer stem cells in solid tumours: accumulating evidence and unresolved questions. Nat. Rev. Cancer *8*, 755–768.

Wicki, A., and Christofori, G. (2007). The potential role of podoplanin in tumour invasion. Br. J. Cancer *96*, 1–5.

Wicki, A., Lehembre, F., Wick, N., Hantusch, B., Kerjaschki, D., and Christofori, G. (2006). Tumor invasion in the absence of epithelial-mesenchymal transition: podoplanin-mediated remodeling of the actin cytoskeleton. Cancer Cell *9*, 261–272.

Yonemura, S., Hirao, M., Doi, Y., Takahashi, N., Kondo, T., and Tsukita, S. (1998). Ezrin/radixin/moesin (ERM) proteins bind to a positively charged amino acid cluster in the juxta-membrane cytoplasmic domain of CD44, CD43, and ICAM-2. J. Cell Biol. *140*, 885–895.

Yuan, P., Temam, S., El-Naggar, A., Zhou, X., Liu, D. D., Lee, J. J., and Mao, L. (2006). Overexpression of podoplanin in oral cancer and its association with poor clinical outcome. Cancer *107*, 563–569.